European Radiology (2019) 29:1565–1573
https://doi.org/10.1007/s00330-018-5702-x

CARDIAC

Correlation of native T1 mapping with right ventricular function and pulmonary haemodynamics in patients with chronic thromboembolic pulmonary hypertension before and after balloon pulmonary angioplasty

F. C. Roller[1] · S. Kriechbaum[2,3] · A. Breithecker[1] · C. Liebetrau[2,3,5] · M. Haas[2,3] · C. Schneider[1] · A. Rolf[2,3,5] · S. Guth[4] · E. Mayer[4] · C. Hamm[2,3,5] · G. A. Krombach[1] · C. B. Wiedenroth[4]

Received: 13 March 2018 / Revised: 20 July 2018 / Accepted: 31 July 2018 / Published online: 29 August 2018

Abstract

Objectives The aim of this study was to assess native T1 mapping in patients with inoperable chronic thromboembolic pulmonary hypertension (CTEPH) before and 6 months after balloon pulmonary angioplasty (BPA) and compare the results with right heart function and pulmonary haemodynamics.

Methods Magnetic resonance imaging at 1.5 T and right heart catheterisation were performed in 21 consecutive inoperable CTEPH patients before and 6 months after BPA. T1 values were measured within the septal myocardium, the upper and lower right ventricular insertion points, and the lateral wall at the basal short-axis section. In addition, the area-adjusted septal native T1 time (AA-T1) was calculated and compared with right ventricular function (RVEF), mean pulmonary arterial pressure (mPAP) and pulmonary vascular resistance (PVR).

Results The mean AA-T1 value decreased significantly after BPA (1,045.8 ± 44.3 ms to 1,012.5 ± 50.4 ms; $p < 0.001$). Before BPA, native T1 values showed a moderate negative correlation with RVEF ($r = -0.61$; $p = 0.0036$) and moderate positive correlations with mPAP ($r = 0.59$; $p < 0.01$) and PVR ($r = 0.53$; $p < 0.05$); after BPA correlation trends were present ($r = -0.21$, $r = 0.30$ and $r = 0.35$, respectively).

Conclusions Native T1 values in patients with inoperable CTEPH were significantly lower after BPA and showed significant correlations with RVEF and pulmonary haemodynamics before BPA. Native T1 mapping seems to be indicative of reverse myocardial tissue remodelling after BPA and might therefore have good potential for pre-procedural patient selection, non-invasive therapy monitoring and establishing a prognosis.

Key Points

- *BPA is a promising treatment option for patients with inoperable CTEPH*
- *Native septal T1 values significantly decrease after BPA and show good correlations with right ventricular function and haemodynamics before BPA*
- *Prognosis and non-invasive therapy monitoring might be supported in the future by native T1 mapping*

Keywords Magnetic resonance imaging · Pulmonary hypertension · Pulmonary embolism · Angioplasty

✉ F. C. Roller
fritz.c.roller@radiol.med.uni-giessen.de

[1] Department of Diagnostic and Interventional Radiology, Justus-Liebig-University Giessen, Klinikstraße 33, 35392 Giessen, Germany

[2] Department of Cardiology, Kerckhoff Heart and Thorax Centre, Bad Nauheim, Germany

[3] DZHK (German Centre for Cardiovascular Research), Partner site Rhein-Main, Frankfurt am Main Germany

[4] Department of Thoracic Surgery Kerckhoff Heart and Thorax Centre, Bad Nauheim, Germany

[5] Department of Cardiology, Justus-Liebig-University Giessen, Klinikstraße 33, Giessen, Germany

Abbreviations

AA-T1	Area-adjusted native T1 time
BPA	Balloon pulmonary angioplasty
CMR	Cardiac magnetic resonance imaging
CTEPH	Chronic thromboembolic pulmonary hypertension
EDD	End-diastolic diameter
EDV	End-diastolic volume
EF	Ejection fraction
ESD	End-systolic diameter
ESV	End-systolic volume
LV	Left ventricle
mPAP	Mean pulmonary arterial pressure
PA	Pulmonary artery
PEA	Pulmonary endarterectomy
PH	Pulmonary hypertension
PVR	Pulmonary vascular resistance
RVEF	Right ventricular function
RVIP	Right ventricular insertion point
RV	Right ventricle
SV	Stroke volume

Introduction

Pulmonary hypertension (PH) is defined as elevation of the mean pulmonary artery (PA) pressure (mPAP) beyond 25 mmHg [1]. Different aetiologies of PH are known and have been categorised according to the Nice classification [2]. Thus, chronic thromboembolic pulmonary hypertension (CTEPH) is defined as PH with persistent perfusion defects after a single or recurrent pulmonary embolism [3]. It is a rare but underdiagnosed disease with an estimated incidence between 0.5% and 3.8% after acute pulmonary embolism and 10% after recurring embolism [4–7]. The persistence of thrombotic material leads to fibrotic obstruction of pulmonary arteries that is compounded by secondary inflammation, cell proliferation and vascular remodelling [8–10]. As a result, elevated mPAP and pulmonary vascular resistance (PVR) ensue, which lead to long-term impairment of right heart function accompanied by poor prognosis and high mortality [11, 12].

CTEPH is potentially curable by surgical pulmonary endarterectomy (PEA) [13–15]. PEA surgery leads to normalisation of pulmonary haemodynamics in most patients [16], and the long-term survival rate is excellent [14]. However, up to one-third of all CTEPH patients are not amenable to surgery, mostly due to the presence of peripherally located lesions [3]. For these patients, targeted medical treatment with riociguat, a stimulator of soluble guanylate cyclase which improves not only pulmonary haemodynamics but also physical capacity of CTEPH patients [17–19], is recommended [8], and balloon pulmonary angioplasty (BPA), an emerging interventional treatment option [8, 20, 21], should also be considered.

Non-invasive assessment with cardiac magnetic resonance imaging (CMR) is widely used to assess RV structure, function and morphology. For example, CMR was used by Kreitner et al [22] and Rolf et al [23] to investigate effects of PEA in CTEPH patients and Van Wolferen et al [24] likewise investigated effects of medical treatment on biventricular heart function in patients with idiopathic PH. Recently, Sato et al [25] and Yamasaki et al [26] investigated effects of BPA in patients with inoperable CTEPH via CMR and showed improvements in biventricular function, pulmonary flow and interventricular dys-synchrony.

Native cardiac T1 mapping provides useful diagnostic information in many cardiac diseases [27–30], permitting parametric tissue characterisation without the need for contrast agents. Initial results in patients with different causes of PH are promising and have shown good correlations with right ventricular function and pulmonary haemodynamics [31–33]. Furthermore, the results of a recent study by Garcia-Alvarez et al [34] in an experimental animal model suggest that native T1 mapping might be suitable as a non-invasive method to assess fibrosis of the upper and lower right ventricular insertion point (RVIP) in chronic PH, as T1 times increase with the degree of fibrosis (myocardial collagen content). In order to determine the potential of native T1 mapping as an imaging biomarker, the aims of our study were to assess native T1 values in patients with inoperable CTEPH before and 6 months after BPA and to examine how well they correlate with right heart function and pulmonary haemodynamics.

Methods

Patient population

A total of 21 consecutive CTEPH patients (12 women) with a mean age of 63.4 ± 10.6 years (± standard deviation [SD]) and a mPAP of 40.9 ± 12.6 mmHg were enrolled in this prospective cohort study from January 2014 to February 2015. The primary diagnosis of CTEPH was based on ventilation-perfusion scintigraphy, right heart catheterisation and biplanar pulmonary angiography. Pre- and post-procedural management of these patients has been recently published [17, 35, 36]. In brief, all patients were assessed by CMR and right heart catheterisation (RHC) as part of their pre-and post-interventional routine workup (assessment of RV function and pulmonary arteries).

Contraindications for CMR and exclusion criteria in all patients were renal failure (glomerular filtration rate below 30 ml/min/1.73 m^2), incompatible cochlear or metallic implants, known gadolinium intolerance, claustrophobia, or the inability to lie supine for the duration of the protocol due to dyspnoea.

All patients gave written informed consent, and the local ethics committee approved the study.

CMR imaging

Imaging was performed with a 1.5-T scanner system (Avanto; Siemens Healthineers, Erlangen, Germany; gradient strength and slew rate: SQ-Engine [45 mT/m at 200 T/m/s]) using a six-element phased array cardiac coil and a dedicated CMR protocol containing axial, coronal, and sagittal thoracic survey images, steady-state-free precession sequences (SSFP) CINE in two-chamber view (CV), three-CV, four-CV and stacked transaxial and short-axis (SA) from base to apex, black-blood (T2 turbo spin echo [TSE]), native T1 mapping and late gadolinium enhancement (LGE) (T1 gradient echo [GE] with inversion recovery) imaging. Gadobenate dimeglumine (Gd-BOPTA; Bracco Imaging, Milan, Italy) was injected at a dose of 0.15 mmol/kg. LGE imaging was performed 12 min after contrast media injection. SSFP imaging parameters were: slice thickness 8 mm; field of view: 300 × 400 mm; matrix 256 × 154; TR 59.62 and TE 1.15. LGE imaging parameters were: slice thickness 8 mm; field of view: 293 × 360 mm; matrix: 256 × 156; TR 843.2 and TE 3.19. Black-blood T2 images were not used for analysis.

The SSFP images were obtained during breath-hold, and the LV and RV systolic and diastolic volumes (absolute values) were calculated from short-axis and transaxial CINE images. Measurements were performed on end-diastolic images (first phase after the R-wave trigger) and end-systolic images (cine with the visually smallest cavity area). Endocardial contours of the LV and RV were obtained by manual tracing with exclusion of papillary muscles and trabeculae from the cavity. Ventricular volumes were estimated using the Simpson rule. The ejection fraction (EF) was calculated as [end-diastolic volume (EDV) – end-systolic volume (ESV)]/EDV**,** end-systolic diameter (ESD), and end-diastolic diameter (EDD) measurements were made using basal short-axis images. The post-processing was performed with the ARGUS software package (Siemens Syngo MMWP Version VE40A; Siemens Healthineers).

T1 mapping images were acquired at basal, mid-ventricular, and apical short-axis sections by using an optimised modified Look-Locker inversion-recovery (MOLLI) sequence, with three images in the first two Look-Locker segments and five images for the third inversion (known as the "3-3-5" standard protocol) [37]. Finally, 11 images were acquired during 17 heartbeats, and in-line motion correction and map generation were performed. Imaging parameters were [32]: slice thickness, 8 mm; spatial resolution, 2.2 mm × 1.8 mm × 8 mm; 6/8 partial Fourier acquisition; field of view, 240 × 340 mm; matrix, 192 × 124; flip angle, 35°; TR, 740; TE, 1.06; TI, 100 ms; TI increment, 80 ms; trigger delay, 300 ms; inversions, 3; acquisition heartbeats, 3, 3, 5; scan time, 17 heartbeats.

Qualitative and quantitative image assessment

All original images were assessed for artefacts due to susceptibility, cardiac, diaphragmatic or respiratory motion. Each motion-corrected series was evaluated for correct image alignment, and each map was carefully checked for signal loss due to misalignment and motion [32].

Image assessment and measurement of native T1

After image acquisition T1 maps were generated after in-line motion correction from the MR workstation [38]. T1 times were measured for myocardium at the basal short-axis section before and after BPA. Basal short-axis slices were chosen to facilitate proper T1 measurements caused by a greater septal myocardial diameter compared to midventricular and apical slices. Thus, a total of four regions of interest (ROIs) were drawn manually at the following locations: septum, upper and lower RVIP, and the lateral wall. ROIs were drawn carefully to exclude the myocardial borders, avoiding partial volume-averaging artefacts and registration errors with gradual T1 value changes that are present at the borders. In addition to the T1 values, the size of the ROIs was also compared and evaluated before and after BPA for each patient to exclude size-dependent differences. Moreover, a total area-adjusted septal native T1 value (AA-T1) was calculated that consisted of the mean T1 values and areas measured for the septum and the RVIPs [32]. The measured T1 values of the septum, the upper and lower RVIP were therefore added up to a sum and divided by the sum of the corresponding ROI areas. All measurements were performed by two experienced radiologists independently (G.K., 20 years of experience, and F.R., 7 years of experience), who were blinded to patient demographics, and LGE assessment was performed blinded to T1 maps and CINE images and vice versa. All studies were used for assessment of inter- and intra-rater variability.

Right heart catheterisation

RHC was performed as a part of the diagnostic workup [8]. RHC was repeated 6 months after the final BPA procedure in all patients. RHC was performed routinely via the right internal jugular vein using a 6-F sheath and a standard Swan-Ganz catheter. The medication of the patients was not modified prior to or during RHC.

Balloon pulmonary angioplasty

As described before [20], BPA was performed as staged procedure under smooth sedation using femoral or jugular access.

Table 1 Demographic data for CTEPH patients before and after BPA

	Pre-BPA	Post-BPA	*p* value
Patients (*n*)	21	21	
Age (years)	58.8 ± 12.2		
Sex (male:female)	9:12		
BSA (m^2)	1.8 ± 0.2		
mPAP (mmHg)	40.9 ± 12.6	34.4 ± 15.4	0.0016
PVR (dyn × s/cm^5)	538.2 ± 246.3	402.6 ± 190.5	0.0001
PCWP (mmHg)	10.3 ± 3.5	9.2 ± 2.6	
CO (l/m)	4.6 ± 1.3	5.0 ± 1.1	0.1649
Treated pulmonary segments (*n*)		10.0 ± 3.2	

Values are mean ± SD or absolute values

BPA balloon pulmonary angioplasty, *BSA* body surface area, *CO* cardiac output, *CTEPH* chronic thromboembolic pulmonary hypertension, *mPAP* mean pulmonary artery pressure, *PCWP* pulmonary capillary wedge pressure, *PVR* pulmonary vascular resistance, *SD* standard deviation

A 6-F sheath (Vista britetip; Cordis, Johnson & Johnson, New Brunswick, NJ, USA) was placed in the pulmonary artery, and a 6-F guiding catheter (in most cases multi-purpose; Medtronic, Minneapolis, MN, USA) was inserted into the pulmonary artery to intubate the target segmental arteries. During the procedure, patients received heparin intravenously to maintain an activated clotting time >250 s. The guide wire (Runthrough NS-PTCA Guide Wire; Terumo, Tokyo, Japan) was placed into the subsegmental arterial branches, passing the obstructing endoluminal material. Subsequently, the subsegmental branches were dilated by multiple inflations of semi-compliant balloons (Emerge™ 2.0/20 mm and 4.0/20 mm; Boston Scientific, Voisins-le-Bretonneux, France). Final fluoroscopy imaging documented the post-procedural morphological results. Expected results were improvement of parenchymal perfusion as well as a quick venous return, which were used to indicate successful intervention. Signs of successful interventions were seen in most patients.

Statistical analysis

Statistical analysis was performed using SPSS statistical software version 20 (SPSS, IBM, Armonk, New York, USA). Patient characteristics were described by mean ± standard deviation (SD). All data were tested for normal distribution using the Shapiro-Wilk test. In cases of normal distribution Student's *t*-test was used, and if the data were not distributed normally the Wilcoxon signed rank test (non-parametric) was used. Intra- and inter-observer variability was tested with simple linear regression analysis. Linear regression analysis was also used for assessing the correlation of native T1 and functional parameters. The correlation coefficient k was interpreted according to Hinkle et al [39], where $r > 0.5$ would be considered a moderate correlation, $r > 0.7$ a strong correlation, and $r > 0.9$ very strong correlation. An $r > 0.5$ would therefore be considered to have clinical impact. Strengths of correlations were tested using the Pearson correlation coefficient. All results were tested at a 5% level of significance and we accepted an alpha error of less than 0.05 as statistically significant.

Results

Table 1 presents patient demographics, RHC measurements and the mean number of treated pulmonary segments. A total of 10.0 ± 3.2 pulmonary segments were treated by BPA per

Table 2 Functional analysis before and after BPA (CMR)

n = 21		Pre-BPA	Post-BPA	*p* value
LV function				
	EF (%)	65.4 ± 10.3	66.5 ± 6.2	0.5603
	EDV (ml)	100.4 ± 24.9	115.4 ± 23.1	0.0187
	ESV (ml)	35.0 ± 13.5	39.3 ± 12.7	0.05
	SV (ml)	65.5 ± 18.4	76.1 ± 13.6	0.0295
	EDD (mm)	42.5 ± 5.8	46.6 ± 4.5	0.0002
	ESD (mm)	24.7 + 6.5	27.5 ± 4.3	0.01
RV function				
	EF (%)	38.2 ± 11.7	47.9 ± 7.6	0.001
	EDV (ml)	191.1 ± 66.3	161.6 ± 52.5	0.0093
	ESV (ml)	124.8 ± 50.2	85.5 ± 38.7	0.0003
	SV (ml)	71.0 ± 17.7	75.9 ± 19.4	0.4168
Wall thickness				
	Septal (mm)	7.3 ± 1.0 mm	7.5 ± 0.9 mm	0.548

Values are mean ± SD or absolute values

BPA balloon pulmonary angioplasty, *CMR* cardiac magnetic resonance imaging, *CTEPH* chronic thromboembolic pulmonary hypertension, *EF* ejection fraction, *EDV* end-diastolic volume, *ESV* end-systolic volume, *SV* stroke volume, *EDD* end-diastolic diameter, *ESD* end-systolic diameter, *LV* left ventricular, *RV* right ventricular

Table 3 Native T1 mapping in CTEPH patients before and after BPA

	Pre-BPA (n = 21) ms	Mean ROI size mm^2	Post-BPA (n = 21) ms	Mean ROI size mm^2	p value
Upper RVIP	1,059.0 ± 49.4	44.6	1,012.1 ± 67.4	37.4	0.0004
Lower RVIP	1,087.9 ± 78.2	38.7	1,062.5 ± 78.9	32.0	0.0637
Septum	1,008.3 ± 41.8	113.3	987.9 ± 40.1	106.8	0.0215
AA-T1	1,045.8 ± 44.3	97.3	1,012.5 ± 50.4	109.4	0.0009
Lateral wall	965 ± 44.3	116.5	972 ± 41.7	114.6	0.43

Values are mean ± SD

BPA balloon pulmonary angioplasty, *CTEPH* chronic thromboembolic pulmonary hypertension, *RVIP* right ventricular insertion point, *AA-T1* area-adjusted T1 time, *ROI* region of interest

patient. The mPAP decreased from 40.9 ± 12.6 mmHg before BPA to 34.4 ± 15.4 mmHg after BPA ($p < 0.01$), and PVR decreased from 538.2 ± 246.3 (dyn × s/cm^5) to 402.6 ± 190.5 (dyn × s/cm^5) ($p < 0.001$). Pulmonary capillary wedge pressure and cardiac output were not significantly affected by BPA.

Pre- and post-procedural LV and RV function as determined by CMR are displayed in Table 2. Before and after BPA all patients had normal LV function regarding EF but stroke volume (SV), EDV and ESV were significantly higher after BPA ($p = 0.0187$, $p = 0.05$ and $p = 0.0295$, respectively). Moreover, BPA resulted in significantly higher RV EF ($p = 0.001$) and significantly lower RV EDV and RV ESV ($p = 0.0093$ and 0.0003, respectively). The RV SV was not significantly different. The end-diastolic and end-systolic LV diameters were significantly higher after BPA ($p = 0.0002$ and 0.01, respectively). Seventeen of the 21 patients (81.0%) displayed typical LGE in the RVIPs pre- and post-procedurally with partially triangular extension to the septum.

The pre- and post-procedural T1 mapping values are presented in Table 3. Significant differences were observed for the septum ($p < 0.05$), the upper RVIP ($p < 0.001$) and for the AA-T1 values ($p < 0.001$), whereas the mean T1 values of the lower RVIP ($p > 0.06$) and the lateral wall ($p = 0.43$) were not significantly different. In addition, the ROIs in all areas measured were not significantly different in size, which means that comparable areas within the myocardium were measured before and after BPA. The inter-observer (upper RVIP, $r = 0.919$; lower RVIP, $r = 0.934$; septum, $r = 0.963$; lateral wall, $r = 0.947$; AA-T, $r = 1$ 0.935; all $p < 0.001$) and intra-observer ($r = 0.937$; $r = 0.939$; $r = 0.976$; $r = 0.939$; $r = 0.956$; all $p < 0.001$) variability for native T1 was very low in all areas.

Figure 1 shows the pre- and post-procedural native T1 maps and corresponding LGE images in a patient who was successfully treated by BPA and demonstrated improved right ventricular function and pulmonary haemodynamics. The T1 measurements were performed within ROIs (white borders) in the native T1 maps pre- and post-BPA and revealed significant decreases for the upper RVIP (1,090 ms to 1,043 ms), for the lower RVIP (1,063 ms to 1,023 ms), for the septum (1,022 ms to 1,005 ms), and for the lateral wall (997 ms to 982 ms). Correlations of native T1 mapping with RV function (RVEF) and pulmonary haemodynamics (mPAP and PVR) are given in Table 4 and corresponding scatter plots are presented in Fig. 2. Before BPA there were moderate significant positive correlations between native T1 values and mPAP ($r = 0.59$; $p < 0.01$) or PVR ($r = 0.53$; $p < 0.05$) and a moderate negative correlation between native T1 values and RVEF ($r =$

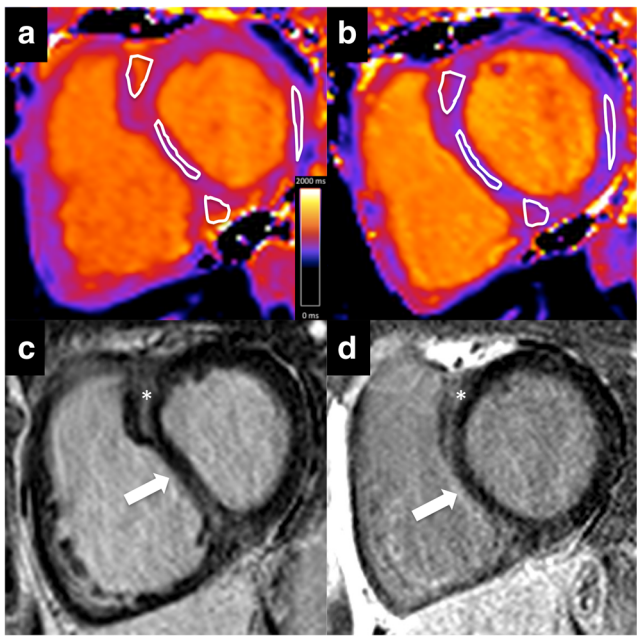

Fig. 1 Native T1 maps and LGE images at basal short axis section in a CTEPH patient pre-and post-BPA. Native T1 maps pre-BPA (**a**) and post-BPA (**b**) and corresponding LGE images pre-BPA (**c**) and post-BPA (**d**) in a 55-year-old man with CTEPH at the basal short-axis level. Pre-procedurally the patient had a mPAP of 51 mmHg at rest and an RVEF of 23.3%. Post-procedurally, mPAP decreased to 35 mmHg and RVEF increased to 45.4%. The patient had a PH-typical LGE pattern in the upper and lower RVIP (*white asterisk*), but the inversed septum receded after BPA (*white arrow*). Consequently, the left and right heart chamber sizes normalised

Table 4 Parameter correlations

	r	CI 95%	*p* value
RVEF to AA-T1			
Pre-BPA	-0.6064	-0.8227 to -0.2367	0.0036
Post-BPA	-0.2105	-0.5887 to 0.2433	0.3596
AA-T1 to mPAP			
Pre-BPA	0.5854	0.2057 to 0.8119	0.0053
Post-BPA	0.3013	-0.1499 to 0.6486	0.1844
AA-T1 to PVR			
Pre-BPA	0.5327	0.1311 to 0.7841	0.0129
Post-BPA	0.3545	-0.0911 to 0.6818	0.1149

Values are mean ± SD or absolute values

BPA balloon pulmonary angioplasty, *mPAP* mean pulmonary artery pressure, *PVR* pulmonary vascular resistance, *RVEF* right ventricular ejection fraction, *SD* standard deviation, *AA-T1* area-adjusted T1 time

-0.61; $r < 0.01$). Six months after BPA these correlations were no longer significant, but a trend towards positive and negative correlation levels still existing ($r = -0.21$, $r = 0.30$ and $r = 0.35$, respectively).

Discussion

To the best of our knowledge, this is the first study to determine the effects of BPA in inoperable CTEPH patients on native T1 time and to correlate the results with RV function and pulmonary haemodynamics. The changes in native T1 times and the moderate correlations with RV function (RVEF) and haemodynamics (mPAP and PVR) in our study are in line with results of previous investigations [31–33]. The increase in RVEF and the decrease in mPAP and PVR were accompanied by significantly decreased T1 times of

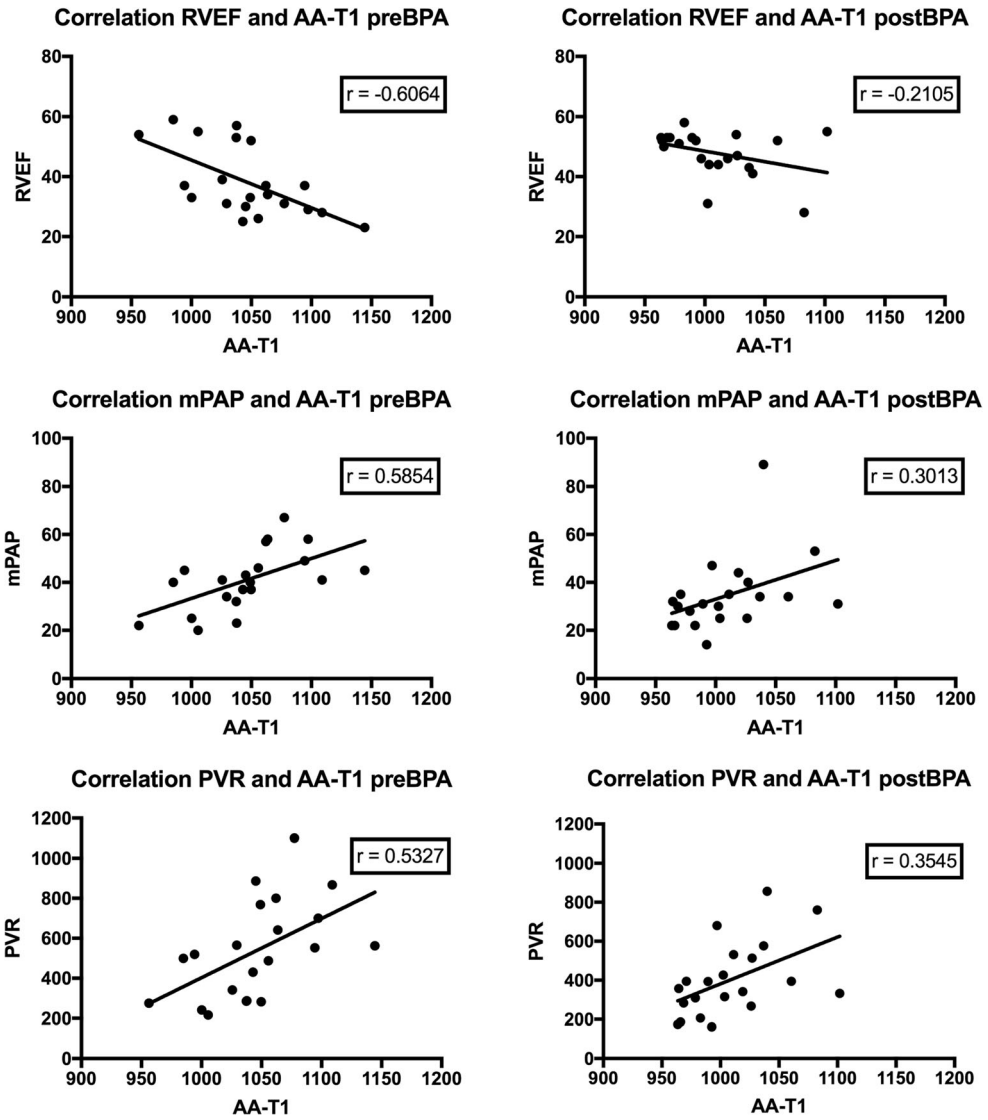

Fig. 2 Scatter plots showing the correlations of AA-T1 to RVEF, mPAP and PVR before and after BPA

the septum, suggesting reverse remodelling of the RV. Septal myocardial remodelling might be explained or rather triggered by possible mechanisms including traction, compression and shear forces due to the RV overload, deterioration and dyskinesia. Normal T1 values could be observed for the RV lateral wall, which therefore might not to be affected [32]. Interestingly, the post-procedural native septal T1 times still correlated weakly with RV function and haemodynamics.

Up to one-third of all CTEPH patients are not eligible for PEA due to the presence of peripherally located lesions [3]. BPA is considered an emerging interventional treatment option for these patients [20, 21, 40]. Non-invasive CMR is useful in PH to assess RV structure, function and morphology. In MRI follow-up studies with CTEPH patients undergoing PEA and BPA, promising results showing enhanced biventricular function and pulmonary flow [25] and improved interventricular dys-synchrony [26] have been reported.

Although improvements in right ventricular function and haemodynamics are well documented for PEA and BPA, little is known about therapy-related cardiac tissue remodelling. LGE in the RVIPs and the septum, which is frequently present in patients with PH [41, 42], is associated with worse outcome in several cardiac diseases [43–46]. However, LGE is only a dichotomous parameter that requires at least 15% of focal matrix expansion to display a myocardial scar [47]; therefore, LGE is limited for characterisation of diffuse tissue alterations, which makes it unsuitable for assessment of treatment effects in diffusely diseased right ventricles. In contrast, mapping techniques (parametric imaging) are increasingly being used within CMR protocols with promising results due to their ability to characterise and to quantify myocardial tissue on a pixel-by-pixel basis.

Native T1 mapping enables characterisation (with characteristics related to the whole myocardium) and visualisation of fundamental myocardial disease processes caused by alterations of tissue composition and structure without the need for contrast agent. Initial results in patients with pre-capillary PH or CTEPH showed good correlations between native T1 mapping and RV function and haemodynamics [31–33]. Since follow-up studies are still lacking, we asked whether the effects of treatment might be assessable via native T1 mapping at the tissue level.

The main limitation of the study is the relatively small number of patients. However, our pre-procedural native T1 mapping results and pre- and post-procedural functional and haemodynamic results are in good agreement with previously published studies [31–33], and experienced cardiac radiologists performed all measurements. Measurement and analysis of post-contrast T1 times and extracellular volume calculation might have provided additional information on the underlying nature of tissue alterations.

Conclusions

Our results suggest two primary conclusions: (1) native T1 measurements of the septal wall reflect tissue alterations that are associated with PH, especially against the background that native T1 values significantly decrease and haemodynamics return to almost normal after successful BPA; (2) BPA not only improves pulmonary arterial haemodynamics but also causes reverse remodelling of the right ventricular myocardium, which is paralleled by improved RV function. These assumptions are based on previous findings that T1 times reflect the myocardial collagen content and hence the degree of fibrosis [34]. Therefore, native T1 mapping holds promise to distinguish patients who will develop reverse remodelling after BPA and those who will not. Further research employing large-scale trials is needed to corroborate these findings.

Acknowledgements We are grateful to Elizabeth Martinson, PhD, from the KHFI Editorial Office for her editorial assistance.

Funding The authors state that this work has not received any funding.

Compliance with ethical standards

Guarantor The scientific guarantor of this publication is Prof. Dr. Gabriele A. Krombach.

Conflict of interest The authors of this manuscript declare no relationships with any companies, whose products or services may be related to the subject matter of the article.

Statistics and biometry One of the authors has significant statistical expertise.

Informed consent Written informed consent was obtained from all subjects (patients) in this study.

Ethical approval Institutional review board approval was obtained.

Methodology
- prospective
- prognostic study/observational/experimental
- performed at one institution

References

1. Hoeper MM, Bogaard HJ, Condliffe R et al (2013) Definitions and diagnosis of pulmonary hypertension. J Am Coll Cardiol 62:42–50
2. Simonneau G, Gatzoulis MA, Adatia I et al (2013) Updated Clinical Classification of Pulmonary Hypertension. J Am Coll Cardiol 62:34–41
3. Pepke-Zaba J, Delcroix M, Lang I et al (2011) Chronic thromboembolic pulmonary hypertension (CTEPH). Results from an international prospective registry. Circulation 124:1973–1981
4. Becattini C, Agnelli G, Pesavento R et al (2006) Incidence of chronic thromboembolic pulmonary hypertension after a first episode of pulmonary embolism. Chest 130:172–175

5. Pengo V, Lensing AW, Prins MH et al (2004) Incidence of chronic thromboembolic pulmonary hypertension after pulmonary embolism. N Engl J Med 350:2257–2264
6. Klok FA, van Kralingen KW, van Dijk AP, Heyning FH, Vliegen HW, Huisman MV (2010) Prospective cardiopulmonary screening program to detect chronic thromboembolic pulmonary hypertension in patients after acute pulmonary embolism. Haematologica 95:970–975
7. Berghaus TM, Barac M, von Scheidt W, Schwaiblmair M (2011) Echocardiographic evaluation for pulmonary hypertension after recurrent pulmonary embolism. Thromb Res 128:e142–e147
8. Galiè N, Humbert M, Vachiery JL et al (2016) 2015 ESC/ERS Guidelines for the diagnosis and treatment of pulmonary hypertension: The Joint Task Force for the Diagnosis and Treatment of Pulmonary Hypertension of the European Society of Cardiology (ESC) and the European Respiratory Society (ERS): Endorsed by: Association for European Paediatric and Congenital Cardiology (AEPC), International Society for Heart and Lung Transplantation (ISHLT). Eur Heart J 37:67–119
9. Lang IM, Pesavento R, Bonderman D, Yuan JX (2013) Risk factors and basic mechanisms of chronic thromboembolic pulmonary hypertension: a current understanding. Eur Respir J 41: 462–468
10. Matthews DT, Hemnes AR (2016) Current concepts in the pathogenesis of chronic thromboembolic pulmonary hypertension. Pulm Circ 6:145–154
11. Riedel M, Stanek V, Widimsky J, Prerovsky I (1982) Longterm follow-up of patients with pulmonary thromboembolism: late prognosis and evolution of hemodynamic and respiratory data. Chest 81: 151–158
12. Lewczuk J, Piszko P, Jagas J et al (2001) Prognostic factors in medically treated patients with chronic pulmonary embolism. Chest 119:818–823
13. Simonneau G, Robbins IM, Beghetti M et al (2009) Updated clinical classification of pulmonary hypertension. J Am Coll Cardiol 54:43–54
14. Mayer E, Jenkins D, Lindner J et al (2011) Surgical management and outcome of patients with chronic thromboembolic pulmonary hypertension: results from an international prospective registry. J Thorac Cardiovasc Surg 141:702–710
15. Lankeit M, Krieg V, Hobohm L et al (2017) Pulmonary endarterectomy in chronic thromboembolic pulmonary hypertension. J Heart Lung Transplant. https://doi.org/10.1016/j.healun.2017.06.011
16. Wirth G, Brüggemann K, Bostel T, Mayer E, Düber C, Kreitner KF (2014) Chronic thromboembolic pulmonary hypertension (CTEPH)—potential role of multidetector-row CT (MD-CT) and MR imaging in the diagnosis and differential diagnosis of the disease. Rofo 186:751–761
17. Ghofrani HA, D'Armini AM, Grimminger F et al (2013) CHEST-1 Study Group. Riociguat for the treatment of chronic thromboembolic pulmonary hypertension. N Engl J Med 369:319–329
18. Simonneau G, D'Armini AM, Ghofrani HA et al (2015) Riociguat for the treatment of chronic thromboembolic pulmonary hypertension: a long-term extension study (CHEST-2). Eur Respir J 45: 1293–1302
19. Simonneau G, D'Armini AM, Ghofrani HA et al (2016) Predictors of long-term outcomes in patients treated with riociguat for chronic thromboembolic pulmonary hypertension: data from the CHEST-2 open-label, randomised, long-term extension trial. Lancet Respir Med 4:372–380
20. Olsson KM, Wiedenroth CB, Kamp JC et al (2017) Balloon pulmonary angioplasty for inoperable patients with chronic thromboembolic pulmonary hypertension: the initial German experience. Eur Resp J 49:6
21. Muller DW, Liebetrau C (2016) Percutaneous treatment of chronic thromboembolic pulmonary hypertension (CTEPH). EuroIntervention 12:X35–X43
22. Kreitner KF, Ley S, Kauczor HU et al (2004) Chronic thromboembolic pulmonary hypertension: Pre- and postoperative assessment with breath-hold MR imaging techniques. Radiology 232:535–554
23. Rolf A, Rixe J, Kim WK et al (2014) Right ventricular adaptation to pulmonary pressure load in patients with chronic thromboembolic pulmonary hypertension before and after successful pulmonary endarterectomy–a cardiovascular magnetic resonance study. J Cardiovasc Magn Reson 16:96
24. van Wolferen SA, Marcus JT, Boonstra A et al (2007) Prognostic value of right ventricular mass, volume, and function in idiopathic pulmonary arterial hypertension. Eur Heart J 28:1250–1257
25. Sato H, Ota H, Sugimura K et al (2016) Balloon pulmonary angioplasty improves biventricular functions and pulmonary flow in chronic thromboembolic pulmonary hypertension. Circ J 80:1470–1477
26. Yamasaki Y, Nagao M, Abe K et al (2017) Balloon pulmonary angioplasty improves interventricular dyssynchrony in patients with inoperable chronic thromboembolic pulmonary hypertension: a cardiac MR imaging study. Int J Cardiovasc Imaging 33:229–239
27. Bull S, White SK, Piechnik SK et al (2013) Human non-contrast T1 values and correlation with histology in diffuse fibrosis. Heart 99: 932–937
28. Lee SP, Lee W, Lee JM et al (2015) Assessment of diffuse myocardial fibrosis by using MR imaging in asymptomatic patients with aortic stenosis. Radiology 274:359–369
29. Dass S, Suttie JJ, Piechnik SK et al (2012) Myocardial tissue characterization using magnetic resonance non contrast T1 mapping in hypertrophic and dilated cardiomyopathy. Circ Cardiovasc Imaging 6:726–733
30. Bandula S, White SK, Flett AS et al (2013) Measurement of myocardial extracellular volume fraction by using equilibrium contrast-enhanced CT: validation against histologic findings. Radiology 269:396–403
31. Reiter U, Reiter G, Kovacs G et al (2017) Native myocardial T1 mapping in pulmonary hypertension: correlations with cardiac function and hemodynamics. Eur Radiol 27:157–166
32. Roller FC, Wiedenroth C, Breithecker A et al (2017) Native T1 mapping and extracellular volume fraction measurement for assessment of right ventricular insertion point and septal fibrosis in chronic thromboembolic pulmonary hypertension. Eur Radiol 27:1980–1991
33. Spruijt OA, Vissers L, Boogard HJ, Hofmann MB, Vonk-Noordegraaf A, Marcus JT (2016) Increased native T1-values at the interventricular insertion regions in precapillary pulmonary hypertension. Int J Cardiovasc Imaging 32:451–459
34. García-Álvarez A, García-Lunar I, Pereda D et al (2015) Association of myocardial T1-mapping CMR with hemodynamics and RV performance in pulmonary hypertension. JACC Cardiovasc Imaging 8:76–82
35. Kriechbaum SD, Wiedenroth CB, Wolter JS et al (2017) N-terminal pro-B-type natriuretic peptide for monitoring after balloon pulmonary angioplasty for chronic thromboembolic pulmonary hypertension. J Heart Lung Transplant. https://doi.org/10.1016/j.healun.2017.12.006
36. Wiedenroth CB, Olsson KM, Guth S et al (2017) Balloon pulmonary angioplasty for inoperable patients with chronic thromboembolic disease. Pulm Circ. https://doi.org/10.1177/2045893217753122
37. Roller FC, Harth S, Schneider C, Krombach GA (2015) T1, T2 mapping and extracellular volume fraction (ECV): application, value and further perspectives in myocardial inflammation and cardiomyopathies. Rofo 187:760–770
38. Kellman P, Wilson JR, Xue H, Ugander M, Arai AE (2012) Extracellular volume fraction mapping inthe myocardium, part 1: evaluation of an automated method. J Cardiovasc Magn Reson 14:63

39. Hinkle DE, Wiersma W, Jurs SG (2003) Applied statistics for the behavioral sciences, 5th edn. Houghton Mifflin, Boston
40. Aoki T, Sugimura K, Tatebe S et al (2017) Comprehensive evaluation of the effectiveness and safety of balloon pulmonary angioplasty for inoperable chronic thrombo-embolic pulmonary hypertension: long-term effects and procedure-related complications. Eur Heart J 38:3152-3159
41. Sanz J, Dellegrottaglie S, Kariisa M et al (2007) Prevalence and correlates of septal delayed contrast enhancement in patients with pulmonary hypertension. Am J Cardiol 100:731–735
42. McCann GP, Beek AM, Vonk-Noordegraaf A, van Rossum AC (2005) Delayed contrast-enhanced magnetic resonance imaging in pulmonary arterial hypertension. Circulation 112:e268
43. Assomull RG, Prasad SK, Lyne J et al (2006) Cardiovascular magnetic resonance, fibrosis, and prognosis in dilated cardiomyopathy. J Am Coll Cardiol 48:1977–1985
44. O'Hanlon R, Grasso A, Roughton M et al (2010) Prognostic significance of myocardial fibrosis in hypertrophic cardiomyopathy. J Am Coll Cardiol 56:867–874
45. Barone-Rochette G, Piérard S, De Meester de Ravenstein C et al (2014) Prognostic significance of LGE by CMR in aortic stenosis patients undergoing valve replacement. J Am Coll Cardiol 64:144–154
46. Krittayaphong R, Saiviroonporn P, Boonyasirinant T, Udompunturak S (2011) Prevalence and prognosis of myocardial scar in patients with known or suspected coronary artery disease and normal wall motion. J Cardiovasc Magn Reson 13:2
47. Moon JC, Reed E, Sheppard MN et al (2004) The histologic basis of late gadolinium enhancement cardiovascular magnetic resonance in hypertrophic cardiomyopathy. J Am Coll Cardiol 43:2260–2264